

# Acid-Catalyzed Reactions of Epoxides for Atmospheric Nanoparticle Growth

Wen Xu,<sup>§</sup> Mario Gomez-Hernandez, Song Guo, Jeremiah Secret, Wilmarie Marrero-Ortiz, Annie L. Zhang, and Renyi Zhang\*

Department of Chemistry and Department of Atmospheric Sciences, Texas A&M University, College Station, Texas 77843, United States

**S** Supporting Information

**ABSTRACT:** Although new particle formation accounts for about 50% of the global aerosol production in the troposphere, the chemical species and mechanism responsible for the growth of freshly nucleated nanoparticles remain largely uncertain. Here we show large size growth when sulfuric acid nanoparticles of 4–20 nm are exposed to epoxide vapors, dependent on the particle size and relative humidity. Composition analysis of the nanoparticles after epoxide exposure reveals the presence of high molecular weight organosulfates and polymers, indicating the occurrence of acid-catalyzed reactions of epoxides. Our results suggest that epoxides play an important role in the growth of atmospheric newly nucleated nanoparticles, considering their large formation yields from photochemical oxidation of biogenic volatile organic compounds.

Aerosols are ubiquitous in the atmosphere and have many consequential effects, such as impairing visibility, modifying the microphysical properties of clouds, altering the Earth's radiation balance, and affecting human health.<sup>1</sup> Currently, the direct and indirect radiative forcings of aerosols represent the largest uncertainty in the projections of future climate. As a key component of atmospheric particulate matter, nanoparticles are frequently formed through gas-to-particle conversion under diverse environmental conditions, including urban, coastal, and forested areas.<sup>1b</sup> New particle formation in the atmosphere involves two consecutive steps, i.e., nucleation to form critical nucleus and growth of freshly nucleated particles to a larger size. The rate of aerosol nucleation is limited by a free energy barrier, which needs to be surmounted before the critical nucleus is formed. In addition, growth of nanoparticles is restricted by the Kelvin (curvature) barrier, because of significantly elevated equilibrium vapor pressures over small particles. Various inorganic and organic species have been identified for their participation in aerosol nucleation,<sup>1b,2,3</sup> including sulfuric acid, basic species, and organic acids. On the other hand, the growth of newly formed nanoparticles is less understood, because of the lack of knowledge in the chemical identities and mechanisms responsible for overcoming the Kelvin barrier.<sup>1b</sup> Several organic compounds have been proposed to contribute to atmospheric nanoparticle growth via particle-phase reactions, such as acid-catalyzed polymerization/oligomeration, hydration, and acid–base reactions. For

example, previous experimental studies have demonstrated that glyoxal and 2,4-hexadienal lead to particle growth for 10 nm and larger sizes, but negligibly for sizes smaller than 4 nm; amines are shown to contribute to nanoparticle growth down to the size of 4 nm.<sup>4</sup> The distinct growth patterns of the different organic species on relative humidity (RH) and particle size have been explained by the reaction mechanisms and the Kelvin effect.<sup>4,5</sup>

Epoxides have been suggested to be produced with a large yield from the oxidation of biogenic hydrocarbons (e.g., isoprene) and to contribute to the formation of secondary organic aerosols (SOA).<sup>6</sup> Isoprene and monoterpenes represent the most abundant volatile organic compounds (VOCs) emitted from the biosphere, with a global emission rate of about 1000 Tg yr<sup>-1</sup>.<sup>7</sup> Epoxides have been shown to be produced from isoprene oxidation in large yields (up to 75%), especially for isoprene epoxydiols.<sup>6c</sup> Also, methacrylic acid epoxide has been suggested to be produced from methacryloylperoxynitrate oxidation (with a yield of 8–32%),<sup>6k</sup> likely explaining SOA formation from isoprene under higher NO<sub>x</sub> conditions.<sup>6b</sup> Recent studies have also indicated that the epoxides derived from 2-methyl-3-buten-2-ol oxidation are important for SOA and organosulfate formation.<sup>6d,m</sup> Epoxide formation from monoterpenes, however, is still debatable. While recent chamber experiments have shown organosulfate formation from reactive uptake of gas-phase epoxides ( $\alpha$ - and  $\beta$ -pinene oxides) by acidic aerosols,<sup>6a</sup> the reactive uptake for  $\alpha$ -pinene oxides has been suggested not to be a major route to formation of aerosols or organosulfates in the atmosphere, since a higher particle acidity is required.<sup>6o</sup>

In the present study, we investigated the growth of sulfuric acid-water nanoparticles from the heterogeneous reactions of epoxides (see Supporting Information (SI)). The size-dependent growth factors of 4–20 nm nanoparticles exposed to three model epoxides (i.e., isoprene oxide,  $\alpha$ -pinene oxide, and butadiene diepoxides) at various RH and reactant concentrations were measured using a nanotandem differential mobility analyzer (n-TDMA). Chemical compositions of the sulfuric acid-water nanoparticles after epoxide exposure were analyzed by using a thermo desorption ion drift chemical ionization mass spectrometer (TD-ID-CIMS).<sup>8</sup> In our experiments, the particle acidity is regulated by RH, and the RH range of 4–68% is relevant to the atmospheric conditions. It should

Received: September 1, 2014

Published: October 22, 2014

be pointed out that in our present work model epoxides, which may not exactly correspond to those produced from atmospheric oxidation biogenic hydrocarbons,<sup>6</sup> are employed. However, the kinetic and mechanistic characteristics of heterogeneous reactions of the model epoxides are likely similar to those for atmospherically relevant compounds, considering the similarity in the molecular functionality (i.e., the epoxide group).

Figure 1 displays an example of the size growth factor for isoprene oxide at various particle mobility sizes and RH. The

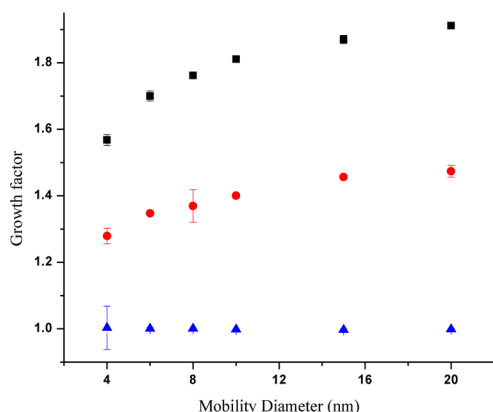


**Figure 1.** Size growth factors, defined by the ratio of the particle size measured after and before the epoxide exposure, of sulfuric acid nanoparticles of various initial sizes exposed to isoprene oxide vapor of  $6 \times 10^{14}$  molecules  $\text{cm}^{-3}$  at 4% (black squares), 43% (red dots), and 68% RH (blue triangles).

measured growth factor of isoprene oxide is dependent on both the RH and particle size: the measured growth factor decreases with increasing RH for a given size but increases with increasing particle size for a given RH. The growth factor ranges from 1.50 to 1.91 at 4% RH but is close to unity at 68% RH. For 43% RH, the growth factors are 1.28 and 1.47 for the particle sizes of 4 and 20 nm, respectively. Similar dependence on RH and particle size is observed for the other two epoxides (Table 1).

**Table 1. Size Growth Factors of 4 and 20 nm Sulfuric Acid Nanoparticles Exposed to Epoxide Vapors at 4% and 30% RH<sup>a</sup>**

species	4 nm		20 nm	
	RH = 4%	RH = 30%	RH = 4%	RH = 30%
isoprene oxide	1.50(0.09)	1.23(0.02)	1.91(0.01)	1.500(0.09)
$\alpha$ -pinene oxide	1.36(0.01)	1.00(0.01)	1.31(0.02)	1.020(0.01)
butadiene diepoxide	1.04(0.01)	1.02(0.01)	1.15(0.05)	1.020(0.02)

<sup>a</sup>Number in the parentheses reflects the  $2\sigma$  standard deviation. The concentrations (in molecules  $\text{cm}^{-3}$ ) are  $6 \times 10^{14}$  for isoprene oxide,  $5 \times 10^{15}$  for  $\alpha$ -pinene oxide, and  $5 \times 10^{16}$  for butadiene diepoxide.

As RH increases from 4% to 30%, the growth factors decrease from 1.15 for butadiene diepoxides and 1.31 for  $\alpha$ -pinene oxide to close to unity. For 20 nm particles, the measured growth factors at 4% RH are 1.15 and 1.31 for butadiene diepoxides and  $\alpha$ -pinene oxide, respectively. The increasing growth factor with increasing particle size is clearly explained by the Kelvin effect.

Figures 2, S2, and S3 depict the TD-ID-CIMS spectra of nanoparticles collected on a platinum filament after the

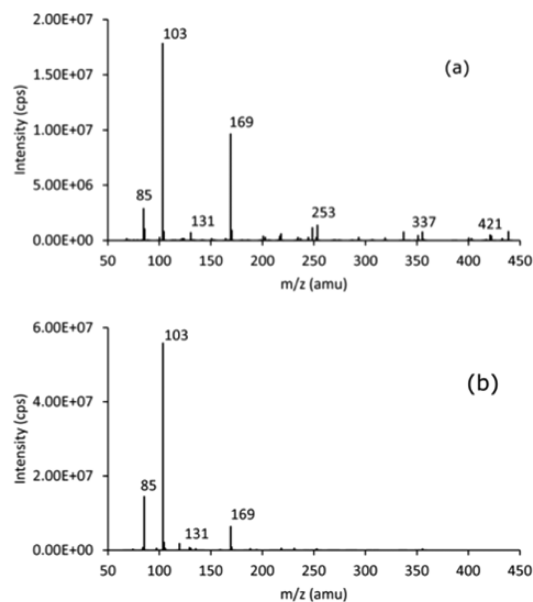
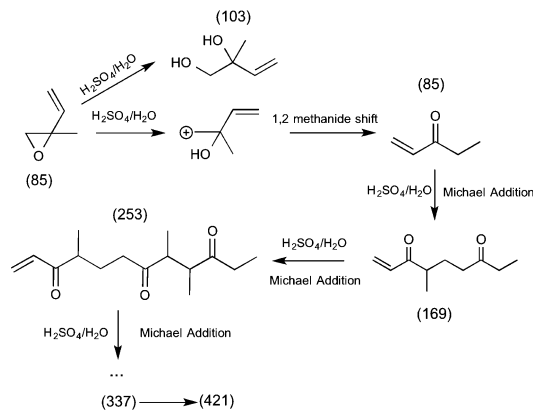


**Figure 2.** (a,b) TD-ID-CIMS spectra of 20 nm sulfuric acid nanoparticles after exposure to isoprene oxide at 4 and 32% RH, respectively.

exposure to isoprene oxide,  $\alpha$ -pinene oxide, and butadiene diepoxides, respectively. The peak assignments for the heterogeneous reactions of epoxides on sulfuric acid nanoparticles are summarized in Table S1. As illustrated in Scheme 1, for the reaction leading to polymerization from isoprene

**Scheme 1. Heterogeneous Reaction Mechanism of Isoprene Oxide on Sulfuric Acid Nanoparticles**



oxide, the  $\alpha,\beta$ -unsaturated ketone formed through 1,2-methanide shift polymerizes via the Michael addition in the presence of sulfuric acid,<sup>9</sup> and the resulting polymers are detected by the TD-ID-CIMS at  $m/z$  of 169, 253, 337, and 421 for dimer, trimer, tetramer, and pentamer, respectively. Organosulfates are not identified for isoprene oxide, since their formation is suppressed by polymerization. In contrast, the previous study by Lal et al.<sup>6h</sup> suggested that the heterogeneous reaction of isoprene oxide in the presence of acid involves protonation and formation of a carbocation, which rearranges into an aldehyde. The reaction mechanism in Schemes S1 and S2 for  $\alpha$ -pinene oxide and butadiene diepoxides is consistent with a previous study.<sup>6a</sup> Because of the absence of the double bond in  $\alpha$ -pinene oxide and butadiene diepoxides, the  $\alpha,\beta$ -unsaturated ketone formation

from both species is implausible, and only organosulfates and dimer are detected at the  $m/z$  peaks of 269 and 305 for  $\alpha$ -pinene oxide and 203 and 209 for butadiene diepoxides, respectively. Hence, our results reveal that, for isoprene oxide, polymers represent the dominant features in the observed mass spectra at different RH, but the formation of organosulfates is noticeably absent. However, for  $\alpha$ -pinene oxide and butadiene diepoxides, formation of organosulfates is most prominent at low RH, but formation of alcohols dominates at high RH. Since polymers and organosulfates are less or nonvolatile,<sup>10</sup> their formation likely explains the measured large growth factors for isoprene oxide measured at different RH and for  $\alpha$ -pinene oxide and butadiene diepoxides measured at low RH. In contrast, alcohols formed from  $\alpha$ -pinene oxide and butadiene diepoxides evaporate into the gas phase, likely explaining the insignificant growth factors at high RH. Hence, the differences in the measured growth factors among the three epoxides can be explained by their respective reaction mechanisms in the particle phase. Interestingly, isoprene-derived epoxydiols have been invoked to explain organosulfate formation in both experimental and field studies,<sup>6</sup> in contrast to isoprene oxide.

Our measured growth factors of sulfuric acid nanoparticles for epoxides can be compared with those previously measured for other organics, including glyoxal, methylglyoxal, 2,4-hexadienal, and trimethylamine under comparable reactant concentrations.<sup>4a</sup> For particles of 4 nm size, the growth factor is only significant for epoxide (isoprene oxide and  $\alpha$ -pinene oxide) and trimethylamine, while the growth factor is close to unity for all other organics. At 4% RH and for 4 nm particles, the growth factors for isoprene oxide (1.50) and  $\alpha$ -pinene oxide (1.36) are much larger than that for trimethylamine (1.10). The occurrence of the particle-phase reaction of trimethylamine on 4 nm particles has been explained by its first-order reaction nature, since reactions of second or higher order are prohibited by the Kelvin effect in the few nanometer size range.<sup>4a</sup> Similarly, polymerization for isoprene oxide and organosulfate formation for  $\alpha$ -pinene oxide are likely of the first-order with respect to the acid concentration,<sup>6f</sup> responsible for their occurrences at 4 nm particles. For 20 nm, the large growth factors for glyoxal are comparable to those for isoprene oxide, except for the opposite trend with RH. The particle-phase reaction for glyoxal involves hydration reaction, followed by oligomerization, in contrast to the acid-catalyzed polymerization for isoprene oxide.

We derive the size-dependent accommodation coefficient ( $\alpha_r$ ) on the basis of the measured growth factor (Figure S4). The accommodation coefficient for the planar surface ( $\alpha_\infty$ ) and characteristic length for Kelvin effect ( $d_o$ )<sup>11</sup> are obtained by nonlinear curve fitting (Table S2). The uptake coefficient of isoprene oxide on the planar sulfuric acid surface at 43% RH is estimated to be  $1.2 \times 10^{-3}$ , which is in the range of the values of  $1 \times 10^{-5}$  to  $3 \times 10^{-3}$  for 3 to 20 wt %  $\text{H}_2\text{SO}_4$  solutions reported by Wang et al.<sup>6i</sup> but smaller than the value of  $1.7 \times 10^{-2}$  reported by Lal et al. on concentrated sulfuric acid (90 wt %  $\text{H}_2\text{SO}_4$ ) surfaces.<sup>6h</sup> A most recent experimental study of the reactive uptake of isoprene-derived epoxydiols on submicron particles has reported the uptake coefficients on ammonium bisulfate (0.05) and ammonium sulfate ( $\leq 1 \times 10^{-4}$ ), showing a similar dependence on acidity as in our present work (i.e., increasing reactivity with increasing acidity).<sup>6p</sup> Also, that study has suggested that the reactive uptake of isoprene-derived epoxydiols on submicron particles may be self-limiting, because of formation of organic coating on the particle surfaces.<sup>6p</sup> Our measured large size growths for the three epoxides on sulfuric

acid nanoparticles, however, do not appear to indicate hindered heterogeneous reactions by organic formation in the particle phase. Considering the possibility of volatile products, which may evaporate from nanoparticles, the uptake coefficient estimated in our present study likely corresponds to a low limit, compared to those previously measured on bulk solutions.<sup>6h</sup> Alcohols have been shown to contribute negligibly to nanoparticle growth;<sup>4b</sup> at 30% RH and 298 K organosulfate formation from methanol takes about 96 h, much longer than the exposure time (ca. 3 s) in our experiment.

Our measurements show that the growth factor increases with increasing concentrations of the epoxides (Figure S5). Since epoxides are typically volatile and their partitioning is highly suppressed because of the curvature effect,<sup>4a</sup> the rate-limiting step in the heterogeneous reactions of epoxides on nanoparticles corresponds to mass accommodation.<sup>4a</sup> Using our measured growth factors (i.e., for isoprene oxide at different concentrations) and at 43% RH and assuming an ambient concentration of epoxides ( $\sim 1$  part per billion), we estimate the growth rates of 0.11 and 1.10 nm h<sup>-1</sup> for 4 and 20 nm particles, respectively, close to those typically measured in the atmosphere.<sup>12</sup> Clearly, the contribution of epoxides to atmospheric nanoparticle growth is dependent on the abundance of the epoxide species, RH, and particle acidity under ambient conditions.

In summary, we have measured the size growth factor of sulfuric acid nanoparticles exposed to three model epoxides, i.e., isoprene oxide,  $\alpha$ -pinene oxide, and butadiene diepoxides. The measured growth factors of the epoxides decrease with increasing RH, reflecting an acid-catalyzed reaction mechanism. The positive correlation between the particle sizes and measured size growth factors on sulfuric acid nanoparticles is explained by the Kelvin effect. Chemical composition analysis of sulfuric acid nanoparticles after epoxide exposure indicates that both  $\alpha$ -pinene oxide and butadiene diepoxides form organosulfates, while isoprene oxide only forms polymers. Organosulfates are formed only in low RH or high acidity conditions, but isoprene-derived polymers are formed in both low and high RH conditions by the acid-catalyzed reaction. The organosulfates and polymers formed from the reactive uptake of epoxides are sufficiently nonvolatile, helping to overcome the Kelvin barrier and contributing to growth of nanoparticles. A lower limit of  $1.2 \times 10^{-3}$  is obtained for the uptake coefficients of isoprene oxide on planar sulfuric acid surface at 43% RH. Our measurements show that the growth factors for isoprene oxide on 4 nm nanoparticles are higher than those previously measured for trimethylamine, glyoxal, and 2,4-hexadienal.<sup>4a</sup> Interestingly, several recent studies have suggested that isoprene suppresses aerosol nucleation events in forested areas.<sup>12</sup> On the other hand, atmospheric measurements have shown efficient new particle formation in urban locations (i.e., southeast US and Beijing, China) with abundant isoprene presence.<sup>13</sup> While the effect of the oxidation products from isoprene on the nucleation free energy is yet to be elucidated, our present results reveal that epoxides likely promote the particle growth by overcoming the curvature barrier. Using our measured growth factor at atmospherically relevant RH (i.e., 43%), we estimate a growth rate of nanoparticles from epoxides that is consistent with those from ambient measurements,<sup>14</sup> indicating that epoxides may contribute significantly to growth of freshly nucleated nanoparticles in the atmosphere. Given the large yield of epoxides from the photochemical oxidation of biogenic VOCs (e.g., isoprene) and their role in new particle

formation, current atmospheric models without inclusion of the epoxide pathway may considerably underestimate the climate forcings of biogenic aerosols.

## ■ ASSOCIATED CONTENT

### 📄 Supporting Information

Experimental details, MS and TDMA data, and analysis. This material is available free of charge via the Internet at <http://pubs.acs.org>.

## ■ AUTHOR INFORMATION

### Corresponding Author

renyi-zhang@tamu.edu

### Present Address

§Aerodyne Research, Inc., 45 Manning Road, Billerica, MA 01821-3976, United States.

### Notes

The authors declare no competing financial interest.

## ■ ACKNOWLEDGMENTS

This work was supported by Robert A. Welch Foundation (Grant A-1417) and U.S. National Science Foundation (AGS-0938352). The authors were grateful to A. Khalizov and L. Wang for assistance with the experimental setup and helpful discussions.

## ■ REFERENCES

- (1) (a) Solomon, S.; Qin, D.; Manning, M.; Chen, Z.; Marquis, M.; Averyt, K. B.; Tignor, M.; Miller, H. L. In *climate change 2007: The physical science basis*, 4th ed.; Cambridge University Press: Cambridge, 2007. (b) Zhang, R.; Khalizov, A.; Wang, L.; Hu, M.; Xu, W. *Chem. Rev.* **2012**, *112*, 1957–2011. (c) Fan, J. W.; Zhang, R. Y.; Li, G. H.; Tao, W. K. *J. Geophys. Res.* **2007**, *112*, D14204.
- (2) Zhang, R. Y. *Science* **2010**, *328*, 1366–1367.
- (3) (a) Zhang, R.; Suh, I.; Zhao, J.; Zhang, D.; Fortner, E. C.; Tie, X.; Molina, L. T.; Molina, M. J. *Science* **2004**, *304*, 1487–1490. (b) Johnston, M. V.; Bzdek, B. R. *Anal. Chem.* **2010**, *82*, 7871–7878. (c) Qiu, C.; Zhang, R. *Phys. Chem. Chem. Phys.* **2013**, *15*, 5738–5752. (d) Bzdek, B. R.; DePalma, J. W.; Ridge, D. P.; Laskin, J.; Johnston, M. V. *J. Am. Chem. Soc.* **2013**, *135*, 3276–3285. (e) Hazra, M. K.; Sinha, A. *J. Am. Chem. Soc.* **2011**, *133*, 17444–17453.
- (4) (a) Wang, L.; Khalizov, A. F.; Zheng, J.; Xu, W.; Ma, Y.; Lal, V.; Zhang, R. Y. *Nat. Geosci.* **2010**, *3*, 238–242. (b) Wang, L.; Xu, W.; Khalizov, A.; Zheng, J.; Qiu, C.; Zhang, R. *J. Phys. Chem. A* **2011**, *115*, 8940–8947.
- (5) Qiu, C.; Zhang, R. *Environ. Sci. Technol.* **2012**, *46*, 4474–4480.
- (6) (a) Iinuma, Y.; Boge, O.; Kahnt, A.; Herrmann, H. *Phys. Chem. Chem. Phys.* **2009**, *11*, 7985–7997. (b) Surratt, J. D.; Chan, A. W. H.; Eddingsaas, N. C.; Chan, M. N.; Loza, C. L.; Kwan, A. J.; Hersey, S. P.; Flagan, R. C.; Wennberg, P. O.; Seinfeld, J. H. *Proc. Natl. Acad. Sci. U.S.A.* **2010**, *107*, 6640–6645. (c) Paulot, F.; Crouse, J. D.; Kjaergaard, H. G.; Kurten, A.; St Clair, J. M.; Seinfeld, J. H.; Wennberg, P. O. *Science* **2009**, *325*, 730–733. (d) Lin, Y. H.; Zhang, Z. F.; Docherty, K. S.; Zhang, H. F.; Budisulistiorini, S. H.; Rubitschun, C. L.; Shaw, S. L.; Knipping, E. M.; Edgerton, E. S.; Kleindienst, T. E.; Gold, A.; Surratt, J. D. *Environ. Sci. Technol.* **2012**, *46*, 250–258. (e) Elrod, M. J.; Minerath, E. C. *Environ. Sci. Technol.* **2009**, *43*, 1386–1392. (f) Elrod, M. J.; Cole-Filipiak, N. C.; O'Connor, A. E. *Environ. Sci. Technol.* **2010**, *44*, 6718–6723. (g) Darer, A. I.; Cole-Filipiak, N. C.; O'Connor, A. E.; Elrod, M. J. *Environ. Sci. Technol.* **2011**, *45*, 1895–1902. (h) Lal, V.; Khalizov, A. F.; Lin, Y.; Galvan, M. D.; Connell, B. T.; Zhang, R. *J. Phys. Chem. A* **2012**, *116*, 6078–6090. (i) Wang, T.; Liu, Z.; Wang, W.; Ge, M. *Atmos. Environ.* **2012**, *56*, 58–64. (j) Bleier, D. B.; Elrod, M. J. *J. Phys. Chem. A* **2013**, *117*, 4223–4232. (k) Lin, Y. H.; Zhang, H. F.; Pye, H. O. T.; Zhang, Z. F.; Marth, W. J.; Park, S.; Arashiro, M.; Cui, T. Q.; Budisulistiorini, H.; Sexton, K.

- G.; Vizuete, W.; Xie, Y.; Luecken, D. J.; Piletic, I. R.; Edney, E. O.; Bartolotti, L. J.; Gold, A.; Surratt, J. D. *Proc. Natl. Acad. Sci. U.S.A.* **2013**, *110*, 6718–6723. (l) Lin, Y.-H. E.; Knipping, M.; Edgerton, E. S.; Shaw, S. L.; Surratt, J. D. *Atmos. Chem. Phys.* **2013**, *13*, 8457–8470. (m) Zhang, H. F.; Worton, D. R.; Lewandowski, M.; Ortega, J.; Rubitschun, C. L.; Park, J. H.; Kristensen, K.; Campuzano-Jost, P.; Day, D. A.; Jimenez, J. L.; Jaoui, M.; Offenberg, J. H.; Kleindienst, T. E.; Gilman, J.; Kuster, W. C.; de Gouw, J.; Park, C.; Schade, G. W.; Frossard, A. A.; Russell, L.; Kaser, L.; Jud, W.; Hansel, A.; Cappellin, L.; Karl, T.; Glasius, M.; Guenther, A.; Goldstein, A. H.; Seinfeld, J. H.; Gold, A.; Kamens, R. M.; Surratt, J. D. *Environ. Sci. Technol.* **2012**, *46*, 9437–9446. (n) Zhang, H. F.; Zhang, H.; Zhang, Z.; Cui, T.; Lin, Y. H.; Bhatela, N. A.; Ortega, J.; Worton, D. R.; Goldstein, A. H.; Guenther, A.; Jimenez, J. L.; Gold, A.; Surratt, J. D. *Environ. Sci. Technol. Lett.* **2014**, *1*, 242–247. (o) Drozd, G. T.; Woo, J. L.; McNeill, V. F. *Atmos. Chem. Phys.* **2013**, *13*, 8255–8263. (p) Gaston, G. J.; Riedel, T. P.; Zhang, J. F.; Gold, A.; Surratt, J. D.; Thornton, J. A. *Environ. Sci. Technol.* **2014**, *48*, 11178–11186.
- (7) Zhang, R. Y.; Wang, L.; Khalizov, A. F.; Zhao, J.; Zheng, J.; McGraw, R. L.; Molina, L. T. *Proc. Natl. Acad. Sci. U.S.A.* **2009**, *106*, 17650–17654.
- (8) Zhao, J.; Zhang, R.; Misawa, K.; Shibuya, K. *J. Photochem. Photobiol. A* **2005**, *176*, 199–207.
- (9) Morrison, R.; Boyd, R. *Organic Chemistry*; 6th ed.; Prentice Hall: Upper Saddle River, NJ, 1992.
- (10) (a) Froyd, K. D.; Murphy, S. M.; Murphy, D. M.; de Gouw, J. A.; Eddingsaas, N. C.; Wennberg, P. O. *Proc. Natl. Acad. Sci. U.S.A.* **2010**, *107*, 21360–21365. (b) Kalberer, M.; Paulsen, D.; Sax, M.; Steinbacher, M.; Dommen, J.; Prevot, A. S. H.; Fisseha, R.; Weingartner, E.; Frankevich, V.; Zenobi, R.; Baltensperger, U. *Science* **2004**, *303*, 1659–1662.
- (11) Lewis, E. R. *J. Aerosol Sci.* **2006**, *37*, 1605–1617.
- (12) Kiendler-Scharr, A.; Andres, S.; Bachner, M.; Behnke, K.; Broch, S.; Hofzumahaus, A.; Holland, F.; Kleist, E.; Mentel, T. F.; Rubach, F.; Springer, M.; Steitz, B.; Tillmann, R.; Wahner, A.; Schnitzler, J. P.; Wildt. *Atmos. Chem. Phys.* **2012**, *12*, 1021–1030.
- (13) (a) Yue, D. L.; Hu, M.; Zhang, R.; Wang, Z. B.; Zheng, J.; Wu, Z. J.; Wiedensohler, A.; He, L. Y.; Huang, X. F.; Zhu, T. *Atmos. Chem. Phys.* **2010**, *10*, 4953–4960. (b) Levy, M.; Zhang, R.; Khalizov, A.; Zheng, J.; Collins, D.; Glen, C.; Wang, Y.; Yu, X. Y.; Luke, W.; Jayne, J.; Olaguier, E. *J. Geophys. Res.* **2013**, *118*, 10,518–10,534.
- (14) Russell, L. M.; Mensah, A. A.; Fischer, E. V.; Sive, B. C.; Varner, R. K.; Keene, W. C.; Stutz, J.; Pszenny, A. A. P. *J. Geophys. Res.* **2007**, *112*, D10S21.